

Title	Integrated Simulation Model between Arc Plasma Process and Weld Mechanics toward Accurate Distortion Analysis : Heat Source Modeling based on Welding Arc Physics
Author(s)	Mochizuki, Masahito; Tanaka, Manabu; Okano, Shigetaka
Citation	Transactions of JWRI. WSE2011 P.123-P.128
Issue Date	2012-03
Text Version	publisher
URL	http://hdl.handle.net/11094/23072
DOI	
rights	

Osaka University Knowledge Archive : OUKA

<https://ir.library.osaka-u.ac.jp/repo/ouka/all/>

Integrated Simulation Model between Arc Plasma Process and Weld Mechanics toward Accurate Distortion Analysis

– Heat Source Modeling based on Welding Arc Physics –

Masahito MOCHIZUKI*, Manabu TANAKA** and Shigetaka OKANO*

* Graduate School of Engineering, Osaka University, 2-1, Yamada-oka, Suita, Osaka 565 0871, Japan

** Joining and Welding Research Institute, Osaka University, 11-1, Mihogaoka, Ibaraki, Osaka 567 0047, Japan

KEY WORDS: (Weld distortion), (Welding heat input conditions), (Numerical simulation), (Heat source modeling), (Welding arc physics)

1. Introduction

Welding has already been established as an essential technology in the fabrication process of objects such as ships, bridges, power plants and automobiles. However, weld distortion is the disadvantages of the welding process from a viewpoint of fabricability and integrity of structures. So, weld distortion should be controlled appropriately. Traditionally, weld distortion has been controlled by weld heat input Q_{net} , which is the heat input per weld length (J/mm). This is because temperature distribution and histories during welding are approximately represented by the weld heat input Q_{net} [1]. The conventional weld heat input Q_{net} , which is calculated as $Q_{net} = \eta IV/v$, is controlled by the following: welding current I and arc voltage V from the welding power source, welding speed v , and arc efficiency η of the welding method.

On the other hand, it is also known that weld distortion is controlled not only by weld heat input, but also by the temperature distributions [2]. This is because temperature distributions, which are for example represented by a weld penetration, become different when the same heat input Q_{net} is used with different combination of weld current, speed and arc voltage. Weld distortion thus changes even at the same heat input conditions. Clearly, a more detailed consideration of the temperature distribution is required for more accurate prediction and control of weld distortion.

In this paper, for more accurate numerical simulation of weld distortion, a procedure is presented for arc physics based heat source modeling from a perspective of heat transfer from arc plasma to a welded plate. The weld heat source model, which is established based on arc plasma simulation, is used for a thermal elastic-plastic analysis. Furthermore, the effect of welding heat input conditions on weld distortion is discussed and verified experimentally. Finally, the effectiveness of heat source modeling based on arc plasma process simulation for the numerical simulation of weld distortion is evaluated.

2. Heat source modeling based on arc plasma simulation

2.1 Simulation model

The process using this model is stationary TIG welding using a tungsten cathode 3.2 mm in diameter with a 60° conical tip. The calculation domain, described in two-dimensional cylindrical coordinates with rotational

symmetry around the arc axis, is shown in Fig. 1. The anode is 490 MPa-class high tensile strength structural steel, JIS SM490YB. Shielding gas is supplied from outside the cathode on the upper boundary at a certain flow rate. Two-dimensional calculations are conducted. Then, the effect of moving of welding torch in two-dimensional axisymmetrical model of stationary TIG welding is virtually considered from a perspective of temperature rise in anode material. This means, thermal energy stored in anode material is deprived with the increase in moving speed of welding torch. The governing equations used in the model are the mass continuity equation, the momentum conservation equation, the energy conservation equation and the current continuity equation. The azimuthal magnetic field induced by the arc current is evaluated by Maxwell's equation. It is necessary to consider the effects of energy transfer at the surfaces of the electrodes. The additional energy fluxes at the cathode and anode are considered. Furthermore, for the cathode surface, the electron current and the ion current are considered separately and defined based on the Richardson-Dushman equation of thermionic emission. The governing and auxiliary equations are solved iteratively by the numerical procedure [3, 4], and the other approximation and boundary conditions are given in previous papers [5-7].

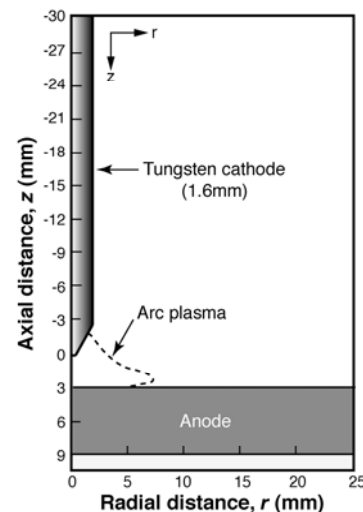


Fig. 1 Calculation domain of arc plasma simulation.

2.2 Evaluation of welding heat input distribution

The welding conditions in the numerical simulation of arc plasma process are shown in Table 1. The welding method is TIG welding. The shielding gas is 100% Ar, and the flow rate is $1.67 \times 10^5 \text{ mm}^3/\text{s}$. To investigate the effect of welding current and welding speed individually, five welding conditions are examined. The base conditions are a 200-A welding current and a welding speed of 1.67 mm/s and a 3-mm arc length. Two approaches for the reduction of weld heat input $Q (= IV / v : \text{J/mm})$ are implemented. One is reducing the welding current (I -changed), and the other is increasing the welding speed (v -changed). These welding conditions are applied in both the 6- and 12-mm plate thicknesses. As the result, the influence of plate thickness is negligibly small.

Table 1 Welding conditions.

	Base	I -changed	v -changed		
Welding current, I (A)	200	160	100	200	200
Welding speed, v (mm/s)	1.67	1.67	1.67	2.33	3.33

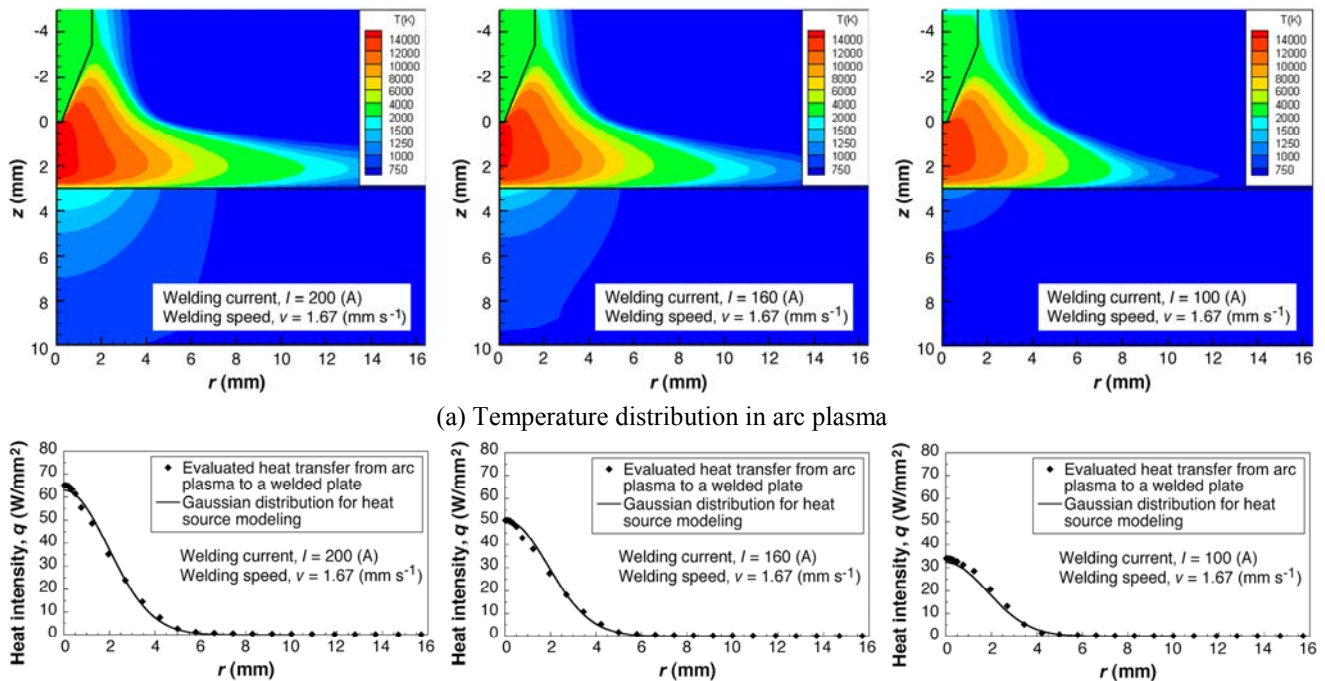
The temperature distributions in TIG arc plasma are shown in Fig. 2(a) and 3(a) for each three cases of varying welding current and welding speed for the 6-mm plate thickness. According to these figures, the temperature distribution in TIG arc plasma is significantly affected by the welding current. When the welding current is 100 A, the spread of the area of increased temperature in the radial

direction is almost within 12 mm. In contrast, when the welding current is 200 A, the spread of the increased temperature area in the radial direction is much greater than 14 mm. The difference in welding speed does not affect either the spread of the increased temperature area in the radial direction in TIG arc plasma. The heat transfer from arc plasma to a welded plate should be considered based on the differences of the temperature distributions in TIG arc plasma due to certain welding conditions. The effect of welding current and speed on the distribution of heat transfer from arc plasma to a welded plate are quantitatively evaluated, as shown in Fig. 2(b) and 3(b). The effects of welding conditions on the heat transfer from arc plasma to a welded plate are summarized as follows: the welding current affects the distribution of heat transfer from arc plasma to a welded plate, the welding speed does not affect the distribution of heat transfer from arc plasma to a welded plate.

2.3 Heat source modeling for distortion analysis

One of the benefits associated with the use of numerical simulation for evaluation of weld distortion is the diversification possible in generating the heat source model for thermal conduction in welding [8-13]. In present, to establish the heat source model from welding conditions, an experiment to obtain information about the weld penetration and temperature profile near the melted zone is imperative. However, a reasonable heat source modeling from the welding conditions should be in nature established based on the consideration of weld physical phenomena.

In this study, the heat source modeling for welding is established based on heat transfer from arc plasma to a welded plate, which was already calculated by the



(a) Temperature distribution in arc plasma
 (b) Distribution of heat transfer from arc plasma to welded plate
 Fig. 2 Effect of welding current on TIG arc plasma.

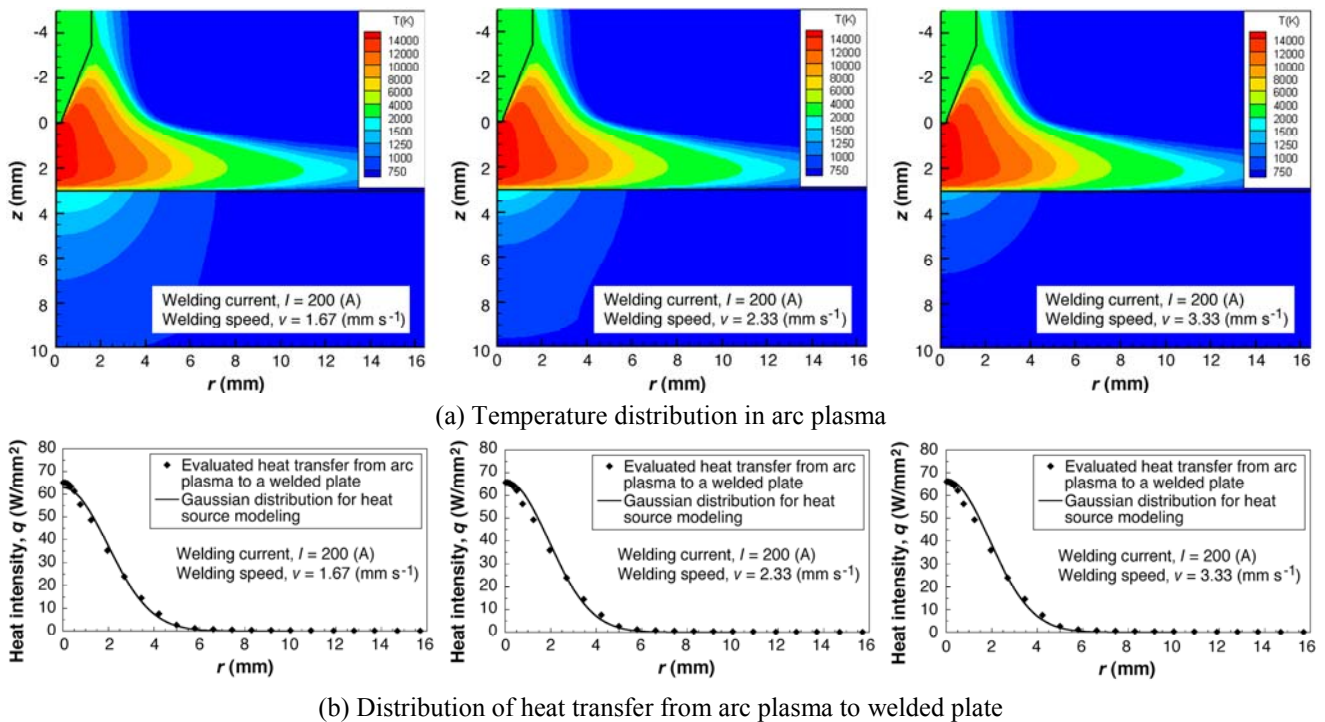


Fig. 3 Effect of welding speed on TIG arc plasma.

numerical simulation of TIG arc plasma. The distribution of heat transfer from arc plasma to a welded plate is approximately expressed by the Gaussian distribution, as follows:

$$w(x,y,t) = \frac{q}{\pi R^2} \exp\left\{-\frac{(x-vt)^2}{R^2}\right\} \exp\left\{-\frac{y^2}{R^2}\right\} \quad (1)$$

where q is weld heat input per time (J/s), R is the radius of the Gaussian distribution and t is time. The weld heat input q and radius of Gaussian distribution R can be determined based on the result of the TIG arc plasma simulation, shown in Table 2. The distribution of heat input in weld heat source used in the numerical simulation of weld residual stress and distortion is also shown in Fig. 2(b) and Fig. 3(b). The Gaussian distribution of the heat input is denoted by a solid line, compared with the distribution of heat transfer obtained by the arc plasma simulation. Both distributions demonstrate good

agreement. Therefore, these distributions are used in the numerical simulation as the heat flux input on the surface.

3. Distortion analysis considering physics of welding arc

3.1 Simulation model

In the thermal elastic-plastic analysis, the simulation model used is bead-on plate model of a 490 MPa-class high tensile strength structural steel, JIS SM490YB, as is shown in Fig. 4. The plate has a length of 200 mm, a width of 500 mm, and a thickness of 6 or 12 mm. The weld length is 150 mm, which leaves un-welded sections of 25 mm at both ends of the plate. Finite element model used is symmetrical model to the weld line due to symmetry of weld phenomena. Work hardening of the material and temperature dependency of the mechanical properties, which include yield stress, Young's modulus and the thermal expansion coefficient, are considered in the mechanical analysis. No restraint is used during the welding process. Details of the mechanical computation

Table 2 Heat source parameter used in distortion analysis.

	Base	<i>I</i> -changed		<i>v</i> -changed	
Welding current, <i>I</i> (A)	200	160	100	200	200
Welding speed, <i>v</i> (mm/s)	1.67	1.67	1.67	2.33	3.33
Weld heat input, <i>q</i> (J/s)	1500	1150	685	1505	1505
Radius, <i>R</i> (mm)	2.8	2.7	2.5	2.8	2.8
Weld heat input, Q_{net} (J/mm)	900	690	410	645	450

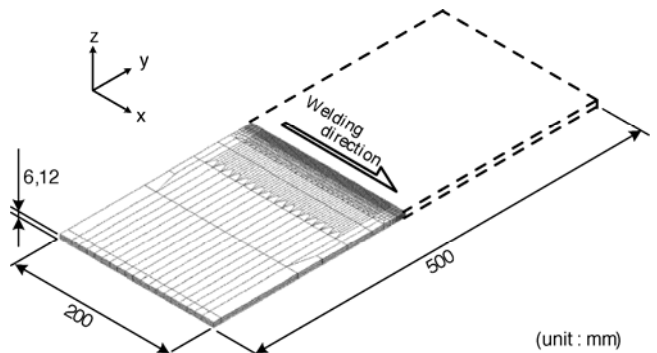


Fig. 4 FE-model used in distortion analysis.

have described in the previous papers [14-18]. As the welding heat source model, above-mentioned heat source model based on welding arc physics is used.

3.2 Effect of welding conditions on weld distortion

Weld distortion are evaluated at center of plate in welding direction. The relationship between the welding conditions and weld distortion is quantified by heat input parameter Q_{net}/h^2 , where h is plate thickness, as is shown in Fig. 5. The heat input parameter is the influential dominant factor of angular distortion theoretically-derived by the similarity rule of the temperature distribution on plate thickness section [19]. Weld distortion is not represented by this heat input parameter. Thus, the difference in the effect of welding current and welding speed on weld distortion becomes clear. When the heat input parameter is small, the weld distortion increases with the increase in welding speed. In contrast, when the heat input parameter is large, the weld distortion decreases with the increase in welding speed.

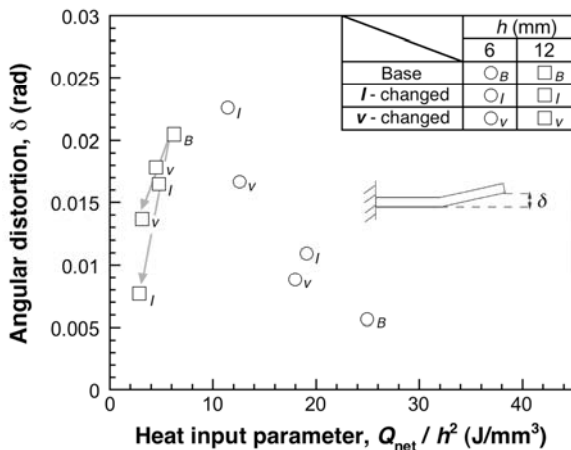


Fig. 5 Effect of welding conditions on weld distortion.

3.3 Experimental verification

Verification of the developed numerical simulation of weld distortion using arc physics based heat source modeling is performed comparing the experimental result of weld distortion with those in numerical simulation. The steel used in the experiment is a 490 MPa-class high tensile strength structural steel, JIS SM490YB. The chemical composition of the steel is shown in Table 3. The configuration of the weld joint used in the experiment is the same as that used in the numerical simulation. The experimental plate is placed on a sill plate because of the heat transfer from the bottom of the welded plate to air. Weld distortion in the experiment is measured by using

Table 3 Chemical compositions of JIS SM490YB (mass%).

Plate thickness (mm)	C	Si	Mn	P	S
6	0.15	0.25	1.42	0.020	0.004
12	0.16	0.28	1.45	0.015	0.003

contact-type displacement gauge in ambient temperature. Welding conditions for the verification experiments are the same as those of the numerical simulation, as is shown in Table 1.

The measured weld distortion in all experimental conditions, including a welding current, a welding speed and a plate thickness, are compared to those simulated; shown in Fig. 6. In the figure, the configuration of weld penetration is also shown in order to compare the experimental results with the simulation results. The penetration shape generated by numerical simulation does not strictly conform to that of the experiment. This is because convective heat transfer in the weld pool is not considered yet in the present numerical simulation. It is known that penetration shape in TIG welding is influenced by convective heat transfer in the weld pool [20-22]. The simulation results however correspond approximately with the experimental results in both weld distortion and penetration. Especially, the weld distortion simulated conforms very closely to that in the experiment. Thus, evaluating the characteristics of weld heat source highly increases the accuracy of predicting the weld distortion. Also, a more detailed understanding of the effects of the

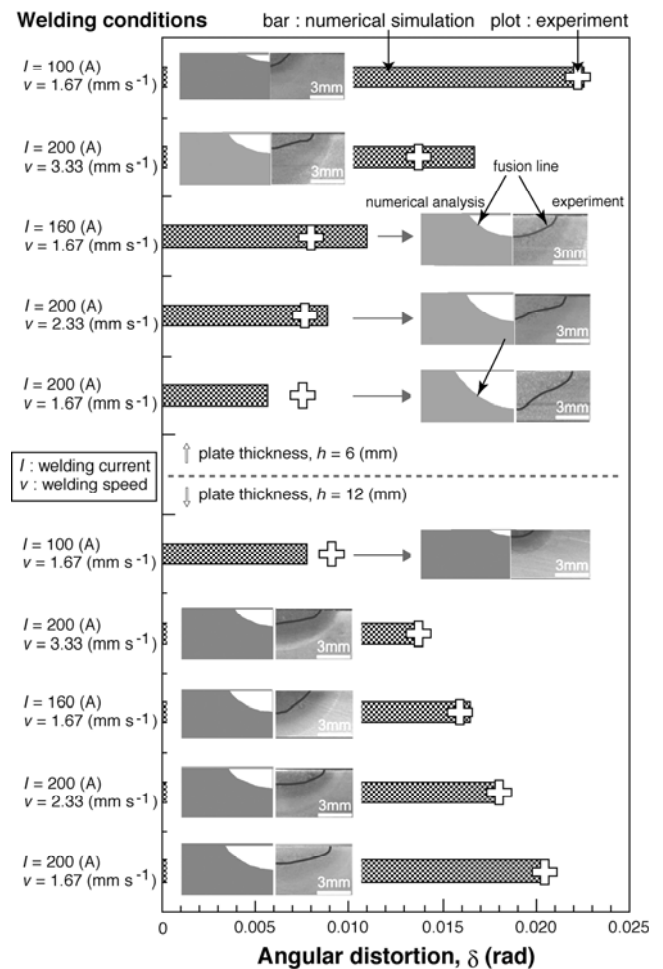


Fig. 6 Comparison of weld distortion between experimental measurement and numerical simulation result.

welding conditions on weld distortion is possible. It can be concluded that the combination of arc plasma simulation and mechanical computation is highly effective in the numerical simulation of weld distortion.

3.4 Arc efficiency

The arc efficiency in TIG arc welding is evaluated considering the effect of welding current and welding speed, as shown individually in Figs. 7(a) and (b). The arc efficiency is calculated by using net weld heat input from numerical simulation of TIG arc plasma, as shown in Table 2, and electrical energy IV/v from welding condition in experiment, as shown in Table 4. According to these figures, arc efficiency in the experiment is approximately 60 to 70%; widely accepted value. The arc efficiency decreases with the increase in welding current; increases slightly, but is generally the same, with the increase in welding speed. Thus, a more detailed understanding of the effects of the welding conditions on arc efficiency also becomes possible.

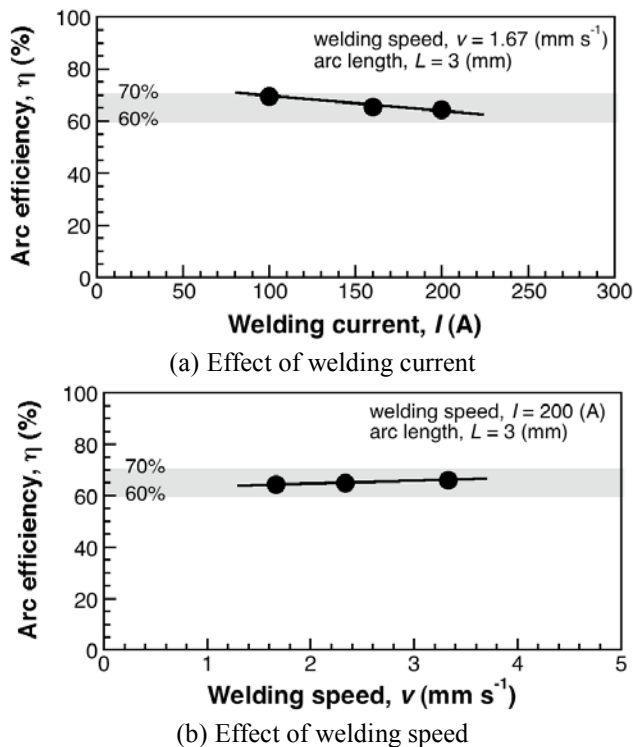


Fig. 7 Effect of welding conditions on arc efficiency.

Table 4 Electrical energy provided in welding experiment.

	Base	I -changed	v -changed		
Welding current, I (A)	200	160	100	200	200
Welding speed, v (mm/s)	1.67	1.67	1.67	2.33	3.33
Arc Voltage, V (V)	11.4	10.6	9.8	11.2	10.6

4. Conclusions

Arc physics based heat source modeling for numerical simulation of weld distortion is studied for more detailed and accurate understanding of the effect of welding conditions on weld distortion. Conclusions reached in this study are as follows:

- (1) For more accurately evaluating the characteristics of heat transfer from arc plasma to a welded plate, numerical simulation of TIG arc plasma is performed. The effects of welding conditions, such as welding current and welding speed, on the distribution of heat input provided to the welded plate are clarified.
- (2) An appropriate heat source modeling for the thermal elastic-plastic analysis is established. Optional parameters, such as heat input and Gaussian radius, are set based on the result of the TIG arc plasma simulation with consideration of weld physical phenomena. The weld penetration simulated by the thermal conduction analysis is almost in good agreement with the experimental configuration measured by macro observation.
- (3) Weld distortion, which is generated by the developed numerical simulation by using the proper heat source modeling, corresponds with that measured in a welding experiment. The developed numerical simulation leads to a more detailed understanding of the effects of welding conditions on weld distortion.
- (4) Arc efficiency in TIG arc welding is calculated as approximately 60 to 70%; a widely accepted value. The effects of welding conditions on arc efficiency are understood more clearly.

Acknowledgements

This study was supported by Priority Assistance for the Formation of Worldwide Renowned Centers of Research – The Global COE Program (Project: Center of Excellence for Advanced Structural and Functional Materials Design), and also a Grant-in-Aid for Scientific Research (B) – No. 20360384, both from the Ministry of Education, Culture, Sports, Science and Technology (MEXT), Japan.

References

- [1] K. Satoh: *J. Jpn. Weld. Soc.*, 1967, 36, (4), 154-159.
- [2] M. Mochizuki, S. Okano, H. Shirai, Y. Hirata and M. Toyoda: *IIW Doc. XII-1925-07*, 2007.
- [3] S. Tashiro, M. Tanaka, K. Nakata, T. Iwao, F. Koshiishi, K. Suzuki and K. Yamazaki: *Sci. Technol. Weld. Joining*, 2007, 12, (3), 202-207.
- [4] S. Tashiro, M. Tanaka, M. Nakatani, M. Furubayashi and Y. Yamazaki: *Q. J. Jpn. Weld. Soc.*, 2007, 25, (1), 3-9.
- [5] M. Ushio, M. Tanaka and J. J. Lowke: *IEEE Trans. Plasma Sci.*, Vol. 32, No. 1, pp. 108-117, 2004.
- [6] M. Tanaka, H. Terasaki, M. Ushio and J. J. Lowke: *Metall. Trans. A*, 2002, 33A, 2043-2052.
- [7] M. Tanaka, H. Terasaki, M. Ushio and J. J. Lowke: *Plasma Chem. Plasma Process*, 2003, 23, 585-606.
- [8] J. Goldak, A. Chakravarti and M. Bibby: *Metall. Trans. B*, 1984, 15B, 299-305.

Integrated Simulation Model between Arc Plasma Process and Weld Mechanics toward Accurate Distortion Analysis

- [9] J. Goldak, M. Bibby, J. Moore, R. Hause and B. Panel: *Metall. Trans. B*, 1986, 17B, 587-600.
- [10] S. Murgan, P. V. Kumar, T. P. S. Gill, B. Raj and M. S. C. Bose: *Sci. Technol. Weld. Joining*, 1999, 4, (6), 357-364.
- [11] Z. Cai, H. Zhao and A. Lu: *Sci. Technol. Weld. Joining*, 2003, 8, (3), 195-204.
- [12] H. X. Wang, Y. H. Wei and C. L. Yang: *Sci. Technol. Weld. Joining*, 2007, 12, (1), 32-44.
- [13] S. Bag and A. De: *Sci. Technol. Weld. Joining*, 2009, 14, (4), 333-345.
- [14] M. Mochizuki, M. Hayashi and T. Hattori: *Trans. ASME J. Eng. Mater. Technol.*, 2000, 122, (1), 98-103.
- [15] M. Mochizuki, H. Yamasaki, S. Okano and M. Toyoda: *Weld. World*, 2006, 50, 46-50.
- [16] M. Mochizuki and M. Toyoda: *Trans. ASME J. Pressure Vessel Technol.*, 2007, 129, (4), 619-629.
- [17] S. Okano, M. Mochizuki and M. Toyoda: *Mater. Sci. Forum*, 2008, 580-582, 585-588.
- [18] Y. Mikami, Y. Morikage, M. Mochizuki and M. Toyoda: *Sci. Technol. Weld. Joining*, 2009, 14, (2), 97-105.
- [19] K. Satoh and T. Terasaki: *J. Jpn. Weld. Soc.*, 1976, 45, (4), 302-308.
- [20] T. Hong, W. Pitscheneder and T. DebRoy: *Sci. Technol. Weld. Joining*, 1998, 3, (1), 33-41.
- [21] J. Jaidi and P. Dutta: *Sci. Technol. Weld. Joining*, 2004, 9, (5), 407-414.
- [22] B. Ribic, R. Rai and T. DebRoy: *Sci. Technol. Weld. Joining*, 2008, 13, (8), 683-693.